JOURNAL OF MATERIALS SCIENCE 29 (1994) 6561–6574

An end-effect model for the single-filament tensile test

E. G. STONER*, D. D. EDIE‡
Department of Chemical Engineering and Center for Advanced Engineering Fibers, Earle Hall, Clemson University, Clemson, SC 29634, USA

S. D. DURHAM
Department of Statistics, University of South Carolina, Columbia, SC 29208, USA

The effect of cross-sectional shape on tensile strength of pitch-based carbon fibres was investigated by extensive single-filament testing. For this study, round and trilobal pitch-based carbon fibres were produced at similar processing conditions. The application of a variety of distributions, including the simple Weibull distribution, to the strength data indicated two sources of failure, one source being the accentuation of end effects at short gauge lengths. A new mixed distribution, the end-effect distribution, was proposed to account for these effects and applied to the experimental data. The end-effect model provided an excellent description of the strength distributions of all fibres studied. The end-effect distribution is not complex and is based on sound physical assumptions. It quantifies a recognized inadequacy of the test method which has not previously been accounted for, and it allows separation of end effects from the true fibre strength distribution. The results indicate that end effects can be an important concern for gauge lengths as long as 40 mm. Use of this model revealed that, in the absence of end effects, all fibres failed due to macroscopic flaws; thus, varying the fibre geometry does not result in an unusual failure mechanism. However, the tensile strengths of the non-circular fibre were found to be less dependent on fibre size. Thus, non-circular fibres can be produced at higher mass flow rates, decreasing filament breakage and increasing process conversions.

1. Introduction

Pitch-based carbon fibres are produced in a three-step process, the first of which consists of melt-extruding the mesophase pitch precursor into fibre form. Then, the as-spun fibres are oxidized or stabilized in air to render them infusible. In the last step, carbonization or graphitization, the stabilized fibres are heated in an inert atmosphere to temperatures greater than 1500 °C to develop the final fibre properties.

The resulting pitch-based carbon fibre is extremely brittle, and as Fig. 1 illustrates, single-filament tensile data exhibit a great deal of scatter. This scatter is a direct result of the various flaws contained in the fibre, flaws which are either present in the precursor material or are introduced during any of the three processing steps. In a study of pitch-based carbon fibres by Jones *et al.* [1], the authors identified a large variety of failure-inducing flaws, including surface damage and/or pitting, mineral inclusions, ferrous particle inclusions from the spinning equipment, elongated voids believed to be due to gas bubbles, and voids which appeared to be the result of inclusions burned off during heat treatment. In addition, there appeared to be little correlation between flaw type and failure stress level, indicating that fibre strength is more dependent on the severity rather than the type of flaw.

Owing to the inherently flaw-limited nature of pitch-based carbon fibres, single-filament tensile strength data obtained from these fibres are difficult to characterize. For example, in research focused on improvements in the tensile strength of pitch-based carbon fibres, preliminary investigations [2, 3] at Clemson University indicated that non-circular fibres were stronger than round fibres of equivalent cross-sectional area. However, the scatter in the tensile test data prevents little more than a comparison of average strengths, and this average strength yields no insight into why one fibre type or shape might be stronger than another.

Fortunately, because the occurrence of flaws within the fibre is random in nature, carbon fibre tensile strength data lend themselves to statistical analysis. Normally, statistical techniques assume that the fibre strength follows some given distributional form, and many of these distributions are based on certain theoretical assumptions concerning the nature of the dominant flaw populations. Thus, by evaluating the fit

* *Present address*: Hoechst Celanese Corp., Charlotte, NC 28232, USA.
† Author to whom all correspondence should be addressed.

0022–2461

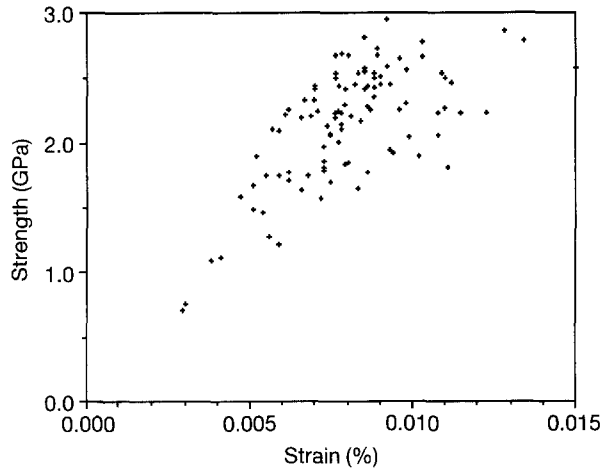

Figure 1 Typical scatter in carbon fibre single-filament tensile data.

of various statistical models to strength data, valuable information concerning the applicability of these assumptions can be obtained.

The work presented here details a model developed as part of an attempt to characterize the single-filament tensile strength of round and trilobal pitch-based carbon fibres. None of the distributions presented in the literature provided a consistent description of the experimental strength data, but the results suggested that the strength data contained test-method related failures, in addition to failures induced by flaws. An end-effect model based on this assumption was developed and found to provide an accurate and consistent description of the observed data.

Before discussing the fit of this and other models to the observed data, it is necessary to have some understanding of the single-filament test method and the data typically obtained for carbon fibres using this method. Therefore, we begin with a background discussion of single-filament testing, as applied to brittle fibres. Then, a number of applicable distributions found in the literature are derived, and the underlying assumptions of each are discussed. In addition, the end-effect model developed in this study will be derived before presenting the results.

The primary focus of this paper is to present the new model for describing pitch-based fibre strength. For details concerning the motivating issue behind the development of the model, the effect of shape on pitch-based fibre strength, the reader is referred to Stoner [4]. Nevertheless, the conditions under which the fibres were produced and tested are briefly detailed in the experimental section.

Finally, the results of applying various distributions to the single-filament test data are presented along with statistical analyses which prove that the end-effect model is superior for describing brittle fibre data. More importantly, the model provides additional insight into the effect of shape on fibre tensile strength.

2. Background

2.1. Single-filament testing

Single-filament testing is a widely used technique for obtaining the tensile strength of materials manufactured in fibre form. For polymeric fibres which exhibit appreciable elongation before failure, the test method is relatively simple because the fibres can be gripped directly by the tensile-testing device. However, brittle fibres such as carbon will shatter if gripped directly, and thus require a different fibre support technique.

The American Society for Testing and Materials (ASTM) describes the acceptable single-filament test method for high-modulus materials [5]. This standard dictates that the fibre first must be mounted on a slotted testing tab, as shown in Fig. 2, with the fibre aligned along the centre of the tab. Glue is used to secure the fibre at opposite ends of the slot, and the tested length of fibre between the glue spots is designated as the gauge length. After the glue has cured, the ends of the tab are grasped by the grips in the upper fixed member and lower moveable member of a tensile-testing device, such as Instron's model TM. The sections of the tab indicated in the figure then are severed so that the fibre is effectively supported only by the grips of the testing device. When the test is initiated, the lower crosshead begins to move downward at a constant speed, straining the fibre until failure occurs.

The calculation of failure stress requires both the breaking load obtained from the tensile testing device and the fibre cross-sectional area. The standard recommends the use of an average cross-sectional area, obtained from measurements of at least 20 fibres in the sampled bundle. While this is acceptable for commercial fibres with comparatively small variations in fibre size, experimental fibres can exhibit appreciable variations in cross-sectional area from fibre to fibre. Therefore, for accurate tensile strength measurements of experimental fibres, it is more appropriate to measure the cross-sectional area of each fibre tested. For round fibres, this measurement can be accomplished through a variety of optical methods, but the measurement of non-circular fibre cross-sectional area is more difficult. The measurement for non-circular fibres requires mounting a segment of the fibre in resin, polishing the cross-section, and measuring the area using a microscope system.

Because carbon fibres fail at extremely low strains, the elongation of the system can dominate the ob-

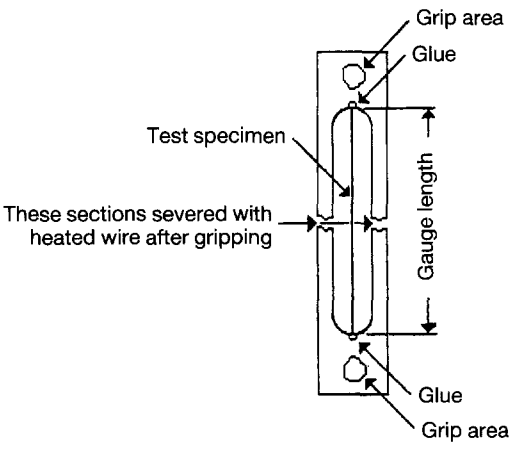

Figure 2 Single-filament testing tab.

served crosshead displacement. To ensure the calculation of reliable failure strain data, the standard test method recommends that system compliance (system elongation per unit load) be accounted for and that a gauge-length to fibre diameter ratio of at least 2000 be utilized in single-filament testing. Failure stress, however, is unaffected by system compliance; thus, when tensile strength is the primary property of interest, carbon fibre data are typically reported at gauge lengths ranging from 0.1–40 mm [1, 6–8].

For carbon fibres, the gauge length utilized is crucial because the average strength decreases as the gauge length increases [1, 6]. This is a direct result of the flaws contained within the fibre; fibres of longer lengths possess a larger number of flaws, and therefore have more potential failure sites and a greater probability of failing at a severe flaw. Thus, the average strength obtained from single-filament testing applies only to the tested gauge length, and the gauge length chosen depends on the purpose of single-filament testing. For example, short gauge lengths have been used to estimate the tensile strength of the fibre critical length, the minimum length of fibre required to ensure adequate load transfer in composite applications [6]; longer gauge lengths are typically used to report accurately failure strain data.

Because of the usefulness of carbon fibre failure at various gauge lengths, statistical techniques often are used to describe the gauge-length dependency of fibre strength. Theoretically, such techniques allow the prediction of average fibre strength at untested gauge lengths. In practice, extrapolation outside the range of the data is always subject to question. Thus, most researchers test at multiple gauge lengths before using these techniques in an effort to obtain as much information as possible concerning the gauge-length dependency of average fibre strength.

A final aspect of pitch-based carbon fibre testing which must be discussed concerns the number of fibres which must be tested to report data. As Fig. 1 illustrates, the flaw-limited nature of the fibre leads to a large variation in the tensile strength. While the data used to prepare this plot were obtained using experimental fibres, commercial fibres also exhibit significant strength variations. As a rule of thumb, analysis of commercial fibre data using a simple two-parameter distribution of fibre strength is rarely reported when less than 30 fibres have been tested, and the use of 50 single-filament tests [6, 8] appears to be an acceptable basis, in practice, for such work.

2.2. Simple Weibull distribution

As previously mentioned, the common approach to analysing fibre tensile strength data involves assuming that the fibre strength follows some given distribution. The most popular distribution is based on the Weibull cumulative distribution function, F, with parameters σ_0 and m [9]

$$F = 1 - \exp\left[-\left(\frac{\sigma}{\sigma_0}\right)^m\right] \quad (1)$$

The cumulative distribution function, F, describes the probability that a fibre will fail at stress level less than or equal to σ. The probability density function, f, of this distribution is

$$f = \frac{m}{\sigma}\left(\frac{\sigma}{\sigma_0}\right)^m \exp\left[-\left(\frac{\sigma}{\sigma_0}\right)^m\right] \quad (2)$$

In Equations 1 and 2, σ_0 and m are the Weibull scale and shape parameters, respectively, and σ is the stress level at which failure occurs. In general, m is inversely related to the variance of σ about its mean value, and σ_0 serves to normalize the variable σ. The mean value of σ, $\bar{\sigma}$, is

$$\bar{\sigma} = \sigma_0\Gamma(1 + 1/m) \quad (3)$$

where Γ represents the gamma function.

There are a variety of distributions other than the Weibull distribution which are commonly used to describe life data, which in this case, refers to the lifetime of a carbon fibre, measured in terms of stress level. Most of these are exponential in nature, and examples include the normal, exponential, and smallest extreme value distributions. The popularity of the Weibull distributions arises from two factors [9]. First, it is often found that the Weibull distribution simply provides a more accurate description of the observed data. In addition, the Weibull probability density function, unlike most others, is flexible in shape. Depending on the value of m, the Weibull density function can reduce to or approximate the shape of various other density functions.

The exact shape of the Weibull probability density function is illustrated in Fig. 3. For values of m between 3.0 and 4.0, the Weibull distribution approximates the normal distribution. When m is unity, the Weibull distribution reduces to the exponential distribution, and when m is 2.0, a distribution called the Rayleigh distribution is obtained.

Thus, when very little information is available concerning the underlying life distribution, the Weibull distribution allows description of the data without imposing stringent assumptions concerning the shape

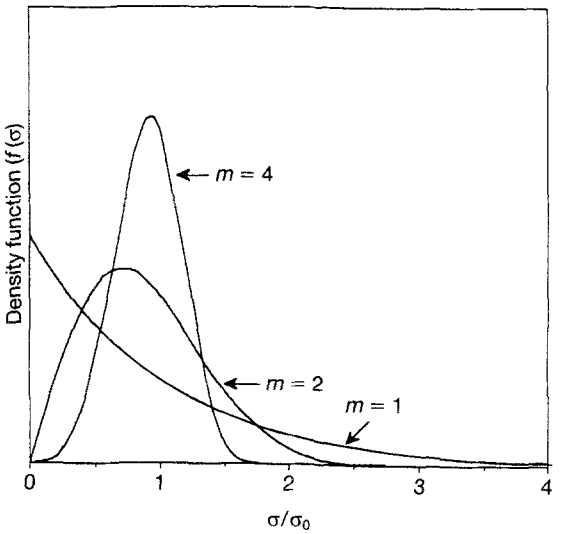

Figure 3 Various shapes assumed by Weibull distribution.

of the unknown density function. The results of fitting a simple Weibull distribution can then be examined to ascertain whether another distribution might be more appropriate, but as already stated, Nelson [9] notes that the Weibull is typically more suitable for describing life data than any of those which it can approximate.

The Weibull distribution has been adapted to specifically account for the gauge-length dependency of the tensile strength of brittle fibres. To illustrate this adaptation, recall that the cumulative distribution function, F, describes the probability that a fibre will fail at or below stress level σ. Because the fibre fails or survives with probability of one at any stress level, the exponential term on the right-hand side of Equation 1 is the probability of fibre survival, S, at stress level σ.

$$S = \exp\left[-\left(\frac{\sigma}{\sigma_0}\right)^m\right] \tag{4}$$

The derivation of the simple Weibull distribution for brittle fibres utilizes this survival probability and weakest link theory [6, 8]. In this derivation, the fibre is assumed to consist of L independent links of arbitrary unit length. The strength of each link is assumed to be identically and independently distributed; that is, the failure or survival of each link is independent of its neighbours, and the strength distribution of each link is a simple Weibull with identical scale and shape parameters. In order for the entire fibre to survive stress level σ, each of the links must also survive. Because the links are independent, the probability that the entire fibre survives is the product of the probabilities that each link survives. Denoting S_i as the probability of survival for link i, this is expressed mathematically as

$$S = \prod_{i=1}^{L} S_i = (S_i)^L = \exp\left[-L\left(\frac{\sigma}{\sigma_0}\right)^m\right] \tag{5}$$

Thus, the adapted Weibull cumulative distribution function used to model fibre strength and the probability density function are given by

$$F = 1 - \exp\left[-L\left(\frac{\sigma}{\sigma_0}\right)^m\right] \tag{6}$$

$$f = \frac{Lm}{\sigma}\left(\frac{\sigma}{\sigma_0}\right)^m \exp\left[-L\left(\frac{\sigma}{\sigma_0}\right)^m\right] \tag{7}$$

The mean strength calculated for this distribution is

$$\bar{\sigma} = \sigma_0 L^{-1/m}\Gamma(1 + 1/m) \tag{8}$$

In applying this distribution to experimental data, the term L is the gauge length at which the fibres were tested.

With the dependency of strength on gauge length explicitly accounted for, the Weibull scale and shape parameters should be constant for all L because, theoretically, a change in L simply increases the number of links in the fibre. The strength of each unit length is assumed to follow the same strength distribution, and because the strength is flaw-limited, the parameters which describe the distribution of strength are also characteristic of the flaw population. The object, then, is to find the scale and shape parameters which most accurately describe the experimentally observed data. A commonly used approach relies on a least-squares fit of a linear form of Equation 6.

$$\ln\ln\left(\frac{1}{1-F}\right) = m\ln(\sigma) + m\ln\left(\frac{L^{1/m}}{\sigma_0}\right) \tag{9}$$

The expression on the right-hand side of Equation 9, commonly called the Weibull quantity, is the dependent variable, while the natural logarithm of the stress level is the independent variable. Thus, m is the slope obtained from a linear regression of the dependent variable on the independent variable, and the scale parameter is calculated using the least-squares intercept and slope. Performing the linear regression requires estimation of the probability of failure, F, because it is not known directly from the raw data. However, the raw data do yield stress levels at which failure occurred, and the probability of failure at or below stress level σ can be estimated as a value approximately equal to the fraction of fibres which failed at or below that stress level.

Another method which can be used to fit the Weibull distribution to experimental data is the maximum likelihood method, in which the likelihood function, l, is the product of the density function evaluated at all gauge lengths and failure stress levels:

$$l = \prod_{i=1}^{N} f_i \tag{10}$$

(where, f_i refers to the density function evaluated at a particular gauge length and stress level, and N is the number of stress levels.) Equivalently, the log-likelihood function, $\mathscr{L}$, can be used, because the likelihood function and its natural logarithm exhibit a maximum at the same parameter values.

$$\mathscr{L} = \sum_{i=1}^{N} \ln f_i \tag{11}$$

To speak in general terms, if f is a function of p parameters, the likelihood function is maximized by calculating the first partial derivative of $\mathscr{L}$ with respect to each of the p parameters. Each derivative is equated to zero, and this leads to p equations with p unknowns.

The linear fit of the Weibull distribution has the advantage of simplicity, and the form of the equation provides a useful means for graphically inspecting the data and comparing various models, even when a least squares approach is not used to fit the parameters. The ML method offers the advantage that a single set of parameters can be determined for all gauge lengths simultaneously; with a least squares approach, the parameters must be determined separately for each gauge length. (If the Weibull distribution is appropriate, the parameters sets for different gauge lengths should be essentially the same.)

The power and popularity of the simple Weibull distribution lie in the ease with which the distribution

can be fit and its flexibility. In addition, the distribution described here accounts explicitly for the effect of gauge length on fibre strength; thus, in theory, it should provide a means for estimating fibre strength at untested lengths. Unfortunately, while the Weibull distribution often provides a good fit to experimental brittle fibre strength data taken at any one gauge length, it rarely gives a consistent description of fibre strength over a range of gauge lengths [6, 7, 10, 11]. For a least squares fit, the parameters often change significantly with gauge length, and as will be seen in the results section, the single set of maximum likelihood parameters often yields a poor fit of the experimental data.

When a simple Weibull distribution seems inappropriate, it might be assumed that the form of the distribution itself is incorrect. However, recall that the shape of this distribution has great flexibility; the simple Weibull distribution is capable of approximating a variety of distributions considered suitable for modelling life data.

Another, more plausible explanation for pitch-based carbon fibres is based on the fact that they are known to possess a variety of different flaw types. Assuming that a simple Weibull distribution is appropriate also implies the assumption that each flaw type affects the tensile strength in the same manner. In other words, it is assumed that all flaws result in one flaw population which gives rise to a simple Weibull distribution of strength. This is not necessarily the case; certain flaws or groups of flaw types acting alone might give rise to Weibull distributions which act over the same stress ranges but have different characteristic shapes. Thus, these flaws or groups of flaw types would comprise a separate flaw population, giving rise to a distinctly different distribution of strength characterized by distinctly different distribution parameters.

By way of example, suppose that there are two flaw populations, each of which, acting alone, gives rise to a simple Weibull distribution of strength, but the parameters which characterize the two strength distributions are significantly different. One unique flaw population might consist of internal flaws within the fibre, while the other might consist of surface flaws. In this case, the cumulative distribution is actually a mixture of the distributions due to each of the two flaw populations, and the use of a simple Weibull distribution is an attempt to combine the effects of four Weibull parameters to obtain a two-parameter model.

If more than one flaw population controls the fibre's tensile strength, a more complex distribution, a mixed distribution, is required to describe properly this situation. The choice of the appropriate mathematical form of the cumulative distribution function depends on how the different flaw populations coexist within the fibre. When the goal of the study is to understand the effect of factors such as gauge length or fibre shape on tensile strength, the formulation and use of the appropriate distribution is particularly crucial in obtaining reliable results.

Obviously, the next level of complexity beyond the simple Weibull distribution is to assume that there are only two distinct, independent (i.e. non-interacting) flaw populations which significantly affect the fibre's tensile strength. Because of the Weibull distribution's flexibility, a reasonable assumption is that each of the populations acting alone gives rise to a simple Weibull distribution of strength. Thus, at least four parameters are required: σ_{01} and m_1, the Weibull scale and shape parameters associated with one flaw population, referred to for convenience's sake as flaw population 1; and σ_{02} and m_2, the Weibull scale and shape parameters associated with the remaining flaw population, or flaw population 2.

Owing to the large amount of data required to adequately estimate several parameters and the tedious nature of the data collection technique, very little work has been presented in the literature concerning mixed strength distributions for brittle fibres. However, Johnson [12] has presented the theoretical formulation of three different distributions to describe life data using a mixture of simple Weibulls. Each of these is based on the assumption that the lifetime distribution of the part (or, in this case, the strength distribution) is controlled by two distinct, independent flaw populations.

In Johnson's work, the differences in the mathematical form of the distributions arise from differences in the assumptions concerning how the flaw populations coexist within the tested part (i.e. the fibre). In the concurrent model, he assumes that each part is subject to both flaw populations 1 and 2. The cumulative distribution function for the exclusive model is based on the assumption that each part contains one of the two flaw populations, but not both. Finally, the cumulative distribution function for the partially concurrent model is derived by assuming that certain parts contain both flaws while the remaining parts contain only one of the two flaw populations. In the partially concurrent model, flaw population 1 is called a background flaw because it is present in all parts.

In each of the models, Johnson [12] assumes that the fibre is subject to two and only two flaw populations. A simple Weibull distribution of strength would result if either of the two were present alone. Thus, the probabilities of survival, S_1 and S_2, at stress level σ associated with flaw populations 1 and 2, respectively, are simple Weibull survival probabilities:

$$S_1 = \exp\left[-L\left(\frac{\sigma}{\sigma_{01}}\right)^{m_1}\right] \quad (12)$$

$$S_2 = \exp\left[-L\left(\frac{\sigma}{\sigma_{02}}\right)^{m_2}\right] \quad (13)$$

The mean values of the strength, $\bar{\sigma}_1$ and $\bar{\sigma}_2$, which would arise from either of two populations acting alone are obtained from Equation 8

$$\bar{\sigma}_1 = \sigma_{01}L^{-1/m_1}\Gamma(1 + 1/m_1) \quad (14)$$

$$\bar{\sigma}_2 = \sigma_{02}L^{-1/m_2}\Gamma(1 + 1/m_2) \quad (15)$$

The derivations of each of these models, in terms which are applicable to brittle fibres, are summarized below, and the implications in using each of these to characterize pitch-based carbon fibre tensile strength are discussed.

2.3. Concurrent model

Because the fibre contains both flaw populations, it must survive both flaw populations if it is to survive stress level σ. Because the flaw populations are independent, the total probability of the fibre survival, denoted as S_T, is the product of the probabilities associated with each flaw population

$$S_T = S_1 S_2 \tag{16}$$

Substitution of Equations 12 and 13 into Equation 16 yields the mathematical expression for the total probability of survival for the fibre at gauge length L and stress level σ

$$S_T = \exp\left[-L\left(\frac{\sigma}{\sigma_{01}}\right)^{m_1} - L\left(\frac{\sigma}{\sigma_{02}}\right)^{m_2}\right] \tag{17}$$

As with the simple model, the cumulative distribution function for the concurrent model, F, is the probability of failure and can be obtained from Equation 17. The density function, f, is the first differential of the cumulative distribution function with respect to σ

$$F = 1 - \exp\left[-L\left(\frac{\sigma}{\sigma_{01}}\right)^{m_1} - L\left(\frac{\sigma}{\sigma_{02}}\right)^{m_2}\right] \tag{18}$$

$$f = \frac{L}{\sigma}\left[m_1\left(\frac{\sigma}{\sigma_{01}}\right)^{m_1} + m_2\left(\frac{\sigma}{\sigma_{02}}\right)^{m_2}\right] \times \exp\left[-L\left(\frac{\sigma}{\sigma_{01}}\right)^{m_1} - L\left(\frac{\sigma}{\sigma_{02}}\right)^{m_2}\right] \tag{19}$$

From a practical standpoint, the assumption that each fibre is subject to both flaw populations seems quite reasonable. Most flaws are introduced during processing, and one would expect that all fibres processed in the same batch would exhibit identical flaw populations. Thus, one might expect this four-parameter model to be quite appropriate in modelling the strength distribution of pitch-based carbon fibres.

2.4. Exclusive distribution

The exclusive distribution is based on the premise that a fraction, x, of the fibre population contains flaw population 1 only, while the remaining fraction, $1 - x$, contains only flaw population 2. Because the fibre can contain only one of two flaw populations, it can survive in two ways. The total probability of survival, S_T, is the sum of the probabilities that (1) the fibre contains and survives flaw population 1, and (2) the fibre contains and survives flaw population 2.

Mathematically, this probability is expressed as

$$S_T = xS_1 + (1 - x)S_2 \tag{20}$$

The cumulative distribution and probability density functions are given below.

$$F = 1 - x\exp\left[-L\left(\frac{\sigma}{\sigma_{01}}\right)^{m_1}\right] - (1 - x) \times \exp\left[-L\left(\frac{\sigma}{\sigma_{02}}\right)^{m_2}\right] \tag{21}$$

$$f = \frac{xLm_1}{\sigma}\left(\frac{\sigma}{\sigma_{01}}\right)^{m_1}\exp\left[-L\left(\frac{\sigma}{\sigma_{01}}\right)^{m_1}\right] + \frac{(1 - x)Lm_2}{\sigma}\left(\frac{\sigma}{\sigma_{02}}\right)^{m_2}\exp\left[-L\left(\frac{\sigma}{\sigma_{02}}\right)^{m_2}\right] \tag{22}$$

This model of the fibre strength distribution requires that five parameters be determined from the experimental data, and from a practical point of view, would not seem applicable to carbon fibres. The assumption that both flaw populations cannot both exist in the same fibre seems questionable at best, and Johnson [12] notes that, in general, one would not expect such a distribution of lifetimes unless samples were taken from parts processed by different methods.

2.5. Partially concurrent distribution

In the partially concurrent model, there are again two flaw populations which, acting alone, give rise to a simple Weibull distribution of strength. Flaw population 1 is common to all the fibres, and a fraction x of the fibres contain only this background flaw. The remaining portion of the fibres $(1 - x)$ contain another distinct flaw population, in addition to the background flaw.

The total survival probability resulting from these assumptions is

$$S_T = xS_1 + (1 - x)\, S_1 S_2 \tag{23}$$

The cumulative distribution and probability density functions for this model are

$$F = 1 - x\exp\left[-L\left(\frac{\sigma}{\sigma_{01}}\right)^{m_1}\right] - (1 - x) \times \exp\left[-L\left(\frac{\sigma}{\sigma_{01}}\right)^{m_1} - L\left(\frac{\sigma}{\sigma_{02}}\right)^{m_2}\right] \tag{24}$$

$$f = \frac{xLm_1}{\sigma}\left(\frac{\sigma}{\sigma_{01}}\right)^{m_1}\exp\left[-L\left(\frac{\sigma}{\sigma_{01}}\right)^{m_1}\right] + \frac{(1 - x)L}{\sigma}\left[m_1\left(\frac{\sigma}{\sigma_{01}}\right)^{m_1} + m_2\left(\frac{\sigma}{\sigma_{02}}\right)^{m_2}\right] \times \exp\left[-L\left(\frac{\sigma}{\sigma_{01}}\right)^{m_1} - L\left(\frac{\sigma}{\sigma_{02}}\right)^{m_2}\right] \tag{25}$$

The partially concurrent model, like the exclusive model, has five parameters. Inspection of Equation 25 reveals that the partially concurrent model reduces to the concurrent model when x is zero, and it is similar in form to the exclusive flaw model. Johnson [12] notes that, for certain parameter values, the partially concurrent model and the exclusive model yield nearly identical descriptions of the experimental data. The assumptions of the partially concurrent model, however, seem more feasible than those of the exclusive model for application to pitch-based carbon fibres.

This finalizes the formulation of the three models proposed by Johnson [12] for describing life-testing or reliability data when it is suspected that two flaw populations are present. In applying these distributions to carbon fibres, one might be tempted to reject

the exclusive flaw model on the basis that the assumptions seem inappropriate. However, the formulation of these various mixed distributions would not be necessary if the researcher knew a priori the nature of the flaw populations and their effect on strength.

The distributions formulated by Johnson [12] are, of course, not the only models which might be formulated to describe life data. For example, Beetz [13] formulated a model based on the exclusive distribution, but he allowed the parameter x, commonly referred to as the mixing parameter, to vary with gauge length. He used this model in conjunction with single-filament data obtained at four gauge lengths, ranging from 6.35–25.4 mm, to describe the strength distribution of carbon fibres. Note that the derivation given above for both the exclusive and the partially concurrent models is still valid if the mixing parameter varies with gauge length, but there would be one mixing parameter for each gauge length tested in addition to four Weibull parameters. For example, because Beetz [13] tested fibres at four gauge lengths, his model contained eight parameters.

Beetz [13] does not clearly indicate why this particular mixed distribution was chosen, and beyond noting that a constant mixing parameter provided a poor description of the experimental data, he does not explore the implications of a mixing parameter which varies with gauge length. However, assuming that the two flaw populations within the fibre exist exclusively, the need to vary the mixing parameter might be justified in at least two special cases. One of the flaw populations might be associated with a flaw which occurs periodically along the fibre, and depending upon the periodicity of the flaw, short gauge lengths might be less likely to contain this flaw than are longer gauge lengths.

On the other hand, the variation in the mixing parameter with gauge length might be the result of the accentuation of end effects at shorter gauge lengths. Recall that the object of the tensile test is to strain the total length of a fibre rigidly fixed at the ends. Undoubtedly, some portion of the fibre near the ends is subject to a complex stress state, and the fraction of the total length subject to end effects increases as the gauge length decreases. Thus, one of the survival probabilities for the two flaw populations might actually be describing the probability that the fibre survives end effects rather than any flaw population contained within the fibre.

Careful examination of Beetz's results [13], listed in Table I, reveals that this might indeed be the case; the flaw population which tends to dominate at low gauge lengths (i.e. has the higher mixing parameter) actually gives rise to a lower probability of survival at any stress level than that which dominates at most longer gauge lengths. In other words, flaw population 1, referred to by Beetz [13] as failure mode 1, dominates at short gauge lengths and yields a lower mean strength. Thus, it is the more severe of the two failure modes. Because it is highly unlikely that the relative contribution of the more severe flaw decreases as gauge length increases, the conclusion that one of the "flaw populations" is the result of a testing artefact seems more feasible than the occurrence of a periodic flaw.

TABLE I Summary of results obtained by Beetz [13] in modelling fibre strength. ($\sigma_{01} = 1.23$; $m_1 = 9.56$; $\sigma_{02} = 0.91$; $m_2 = 4.94$)

Gauge length, L (mm)	x	$\bar{\sigma}_1$ (GPa)	$\bar{\sigma}_2$ (GPa)
6.35	1.00	2.03	2.33
12.70	0.92	1.89	2.02
19.05	0.46	1.81	1.86
25.40	0.81	1.76	1.76

Beetz [13] did not come to this same conclusion in his work, and therefore, did not attempt to develop a more consistent model based on the results. When the data obtained in the current work were analysed using each of the distributions developed above, the results were quite similar to those obtained by Beetz [13]. These findings, presented in Section 4, led to the development of the end-effect model, which is based on the assumption of one dominant flaw population. However, the strength distribution is also assumed to be affected by failures caused by stress concentration at the fixed ends. This model is derived below.

2.6. End-effect model

Assuming stress concentrations near the end of the fibre, some fibres are likely to fail due to the testing technique rather than the flaw population alone. Because the cause of failure cannot be identified, those fibres which failed due to end effects can not be deleted from the experimental data. Thus, one specification was that the model must account for such failures. (Hereafter, end effects will be referred to as a failure mode. Obviously, they do not comprise a conventional flaw population.)

In addition, any fibre tested by a single-filament tensile test will be subject to end effects, although longer gauge lengths would be less susceptible to end-effect related failures. Each fibre is also subject to failure due to the effects of the true flaw population(s). Thus, another aspect of the model was specified: the survival probabilities associated with end effects and flaw populations must act concurrently to determine the total probability of survival.

Keeping the model as simple as possible is always desirable; therefore, it was assumed that the effects of all true flaws on the fibre strength distribution could be represented by a single, simple Weibull distribution of strength, based on weakest link theory. Therefore, the survival probability, S_1, associated with flaws in the fibre is identical in form to that given earlier for the concurrent, exclusive, and partially concurrent distributions

$$S_1 = \exp\left[-L\left(\frac{\sigma}{\sigma_{01}}\right)^{m_1}\right] \quad (26)$$

Because the Weibull distribution is flexible in shape, this distribution was also used to describe end effects. However, the gauge-length dependency derived earlier

is not applicable here, because it dictates that end effects act over the entire length of fibre. End effects only apply to some region of the fibre near the glue spots; therefore, a slightly different adaptation of the basic Weibull distribution defined in Equation 1 was required.

The survival probability associated with end effects is based on the assumption that a region of length $\delta/2$ at each end of the fibre adjacent to the glue spots is subject to end effects. Load can be carried in these regions, but the stress concentrations at the fibre–glue interface give rise to a complex stress state in these regions. This results in a significantly different distribution of strength from that associated with the true flaw population. The total length of fibre subject to end effects is δ, and there is no justification for assuming that δ varies with gauge length. Because δ can also be considered to represent the number of individual links subject to end effects, the weakest link theory can be used to derive the survival probability associated with end effects

$$S_2 = \exp\left[-\delta\left(\frac{\sigma}{\sigma_{02}}\right)^{m_2}\right] \quad (27)$$

However, because neither δ nor σ_{02} change with gauge length, the two parameters cannot be uniquely determined. Thus, in developing this model, the combination of these two parameters was represented by σ_{02}, and δ was dropped as a separate parameter

$$S_2 = \exp\left[-\left(\frac{\sigma}{\sigma_{02}}\right)^{m_2}\right] \quad (27)$$

Because the fibre must survive both end effects and the true flaw population if it is to survive stress level σ, the total probability of survival is obtained in the same manner as that in the concurrent flaw model

$$S_T = S_1 S_2 \quad (28)$$

The cumulative distribution and density functions for this model, referred to as the end-effect model, are given in Equations 29 and 30, respectively

$$F = 1 - \exp\left[-L\left(\frac{\sigma}{\sigma_{01}}\right)^{m_1} - \left(\frac{\sigma}{\sigma_{02}}\right)^{m_2}\right] \quad (29)$$

$$f = \left[\frac{L\sigma^{(m_1-1)}}{\sigma_{01}^{m_1}} + \frac{\sigma^{(m_2-1)}}{\sigma_{02}^{m_2}}\right] \times \exp\left[-L\left(\frac{\sigma}{\sigma_{01}}\right)^{m_1} - \left(\frac{\sigma}{\sigma_{02}}\right)^{m_2}\right] \quad (30)$$

The form of this distribution, which has four parameters, is nearly identical to that of the concurrent distribution, but the failure mode associated with end effects is not gauge-length dependent.

Each of the models detailed in this section was used in an attempt to describe the strength distributions of round and trilobal fibres tested over a range of gauge lengths. As will be seen, the end-effect model, which is based on simple assumptions and accounts for a known inadequacy of the test method, provided the only adequate and consistent description of the experimental data. Before these results are presented, the experimental techniques used to produce these fibres will be discussed, as well as the bases used to compare the two different fibre shapes.

3. Experimental procedure

In this work, the tensile strengths of round and trilobal fibres were compared, and Fig. 4 illustrates the two bases used to compare the two shapes. In the equivalent area study, the two shapes possess equivalent volumes in which flaws can exist. In the equivalent thickness study, the diameter of the as-spun round fibre was equivalent to the thickness of the central portion of the limb of the trilobal fibre. The basis for the latter study was chosen to ensure equivalent heat-treatment conditions for the two shapes, because previous experience with large round fibres indicated that the effectiveness of the oxidation step can be limited by the distance through which oxygen must penetrate to stabilize the fibre.

The precursor pitch was a heat-soaked mesophase, prepared according to the method given by Singer [14]. For details on the equipment, procedures and exact conditions used to melt spin and heat treat all fibres, the reader is referred to Stoner [4]. Briefly, a pilot-scale extruder was used to melt spin the precursor into fibre form at temperatures ranging from 342–354 °C, depending on the fibre shape and spinnerette used.

Oxidation and carbonization were conducted in a batch fashion. A typical temperature profile for the oxidation oven is shown in Fig. 5. At 180 °C an in-

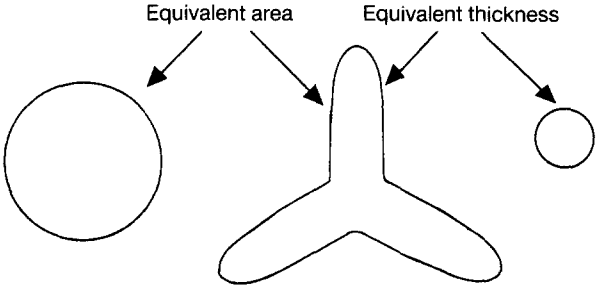

Figure 4 Bases of comparison for round and trilobal carbon fibres.

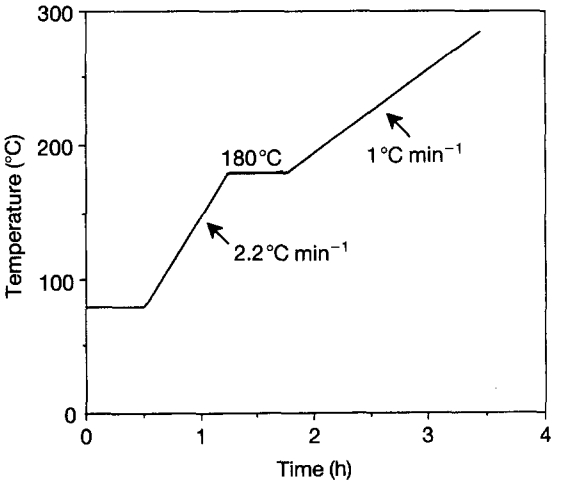

Figure 5 Typical oxidation profile for round and trilobal pitch-based fibres.

crease in bundle mass indicates the onset of oxidation, and all profiles employed a 30 min soak at 180 °C followed by a 1 °C min^{-1} temperature ramp until a mass gain of from 6%–8% was indicated.

In carbonization, the fibres were heated to 1000 °C at a rate of 20 °C min^{-1} to allow the slow evolution of light gases. For round and trilobal fibres of equivalent area, this heating rate was maintained to the final carbonization temperature of 1900 °C. Improvements in the furance allowed the use of a much higher heating rate, approximately 63 °C min^{-1}, in heating round and trilobal fibres of equivalent thickness from 1000 °C to the final carbonization temperature of 2400 °C. All fibres were held at the final temperature for 10 min.

After carbonization, the fibres were subjected to single-filament testing, according to the standard described earlier, at gauge lengths of 10, 20, and 40 mm. For each fibre type and at each gauge length, approximately 100 single-filament breaks were obtained on a Phoenix tensile testing device, a computerized test system built around an Instron model TM. The fibres were glued to the test tabs with excess fibre trailing off the ends, and a small section of the excess length was retained for cross-sectioning purposes prior to single-filament testing.

For round fibres, the diameter of the fibre was measured using an optical microscope equipped with a calibrated scale on the eyepiece. For trilobal fibres, it was not feasible to measure the cross-sectional area of a section within the tested gauge length. This was because carbon fibres typically shatter upon failure, leaving no segments for use in cross-sectional area determination. However, this problem was overcome by retaining a segment of the fibre adjacent to that mounted for single-filament testing. This section was embedded in epoxy and the sample polished to obtain a smooth cross-section. Then, the cross-sectional areas of these segments were measured using a microscope in conjunction with an image analysis system.

All of the distributions discussed previously were fit to the experimental data using the maximum likelihood method. The computer program used the first derivatives of the log-likelihood function, initial guesses input by the user, and a downhill simplex method to find the parameters which maximized the log-likelihood function (hereafter referred to simply as the likelihood function).

As previously noted, a plot of the Weibull quantity (see Equation 9) versus the natural logarithm of the stress level is a convenient way to examine the data. These two quantities can be calculated given the parameters of any of the distributions of interest. Because this plot gives a common basis for graphical comparison of the fits of distributions based on different assumptions, it is used to present the results in the following sections. In addition, the value of the maximum likelihood function (MLF) will be given for each fit, because larger MLF values indicate better fits of the experimental data.

TABLE II Average fibre properties for various round and trilobal fibres

Fibre shape	Study	Gauge length (mm)	Strength (GPa)	Cross-sectional area (μm^2)
Round	Equivalent area*	10	2.15	114.8
		20	2.04	116.1
		40	1.95	114.0
Trilobal	Equivalent area*	10	1.75	186.5
		20	1.65	183.7
		40	1.52	185.6
Round	Equivalent thickness	10	2.16	70.0
		20	1.94	67.6
		40	1.84	67.6
Trilobal	Equivalent thickness	10	1.75	363.2
		20	1.59	373.9
		40	1.47	364.0

* As-spun cross-sectional areas of round and trilobal fibres were equivalent.

TABLE III MLF values of various models used to describe round and trilobal fibre tensile data

Model/no. of parameters	Round equivalent area MLF value	Trilobal equivalent area MLF value	Round equivalent thickness MLF value	Trilobal equivalent thickness MLF value
Simple Weibull/2	− 216.7	− 155.2	− 303.4	− 272.4
Concurrent/4	− 213.9	[a]	− 302.7	− 265.0
Exclusive/5	− 207.8	− 148.5	− 289.8	− 256.5
Partially concurrent/5	− 205.7	− 149.1	− 289.4	− 255.1
Exclusive, varying x/7	− 195.7	− 145.9	− 282.1	− 251.1
End-effect/4	− 195.3	− 147.4	− 282.9	− 248.9

[a] No unique parameter set found.

4. Results and discussion

Table II presents the average fibre properties for the various fibre types utilized in this study, and Table III gives the MLF values for the various models fit to the experimental data. In Table III, each model was fit using data at all gauge lengths simultaneously to obtain a single set of model parameters, and the MLF value was computed in the same fashion. The entry "exclusive model, varying x" in Table III corresponds to the model used by Beetz, and will be discussed in more detail below.

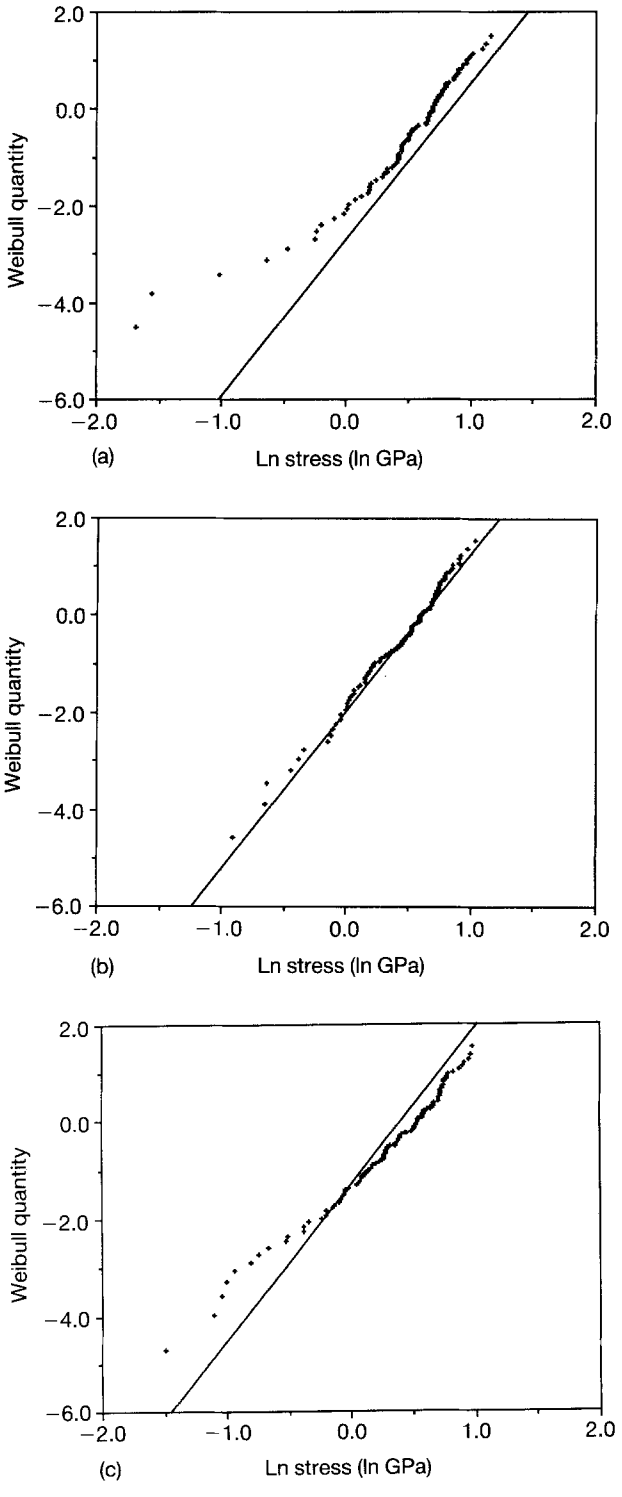

Figure 6 Simple Weibull distribution fit to trilobal fibre data, equivalent thickness study: (a) 10 mm gauge length; (b) 20 mm gauge length; (c) 40 mm gauge length.

Only one fibre type, trilobal fibres from the equivalent thickness study, will be used to illustrate the fit of the simple Weibull distribution and various models proposed by Johnson [12], for the following reasons: first, it would not be feasible to present the fits for each model, gauge length, and fibre type studied, and more importantly, Johnson's models provided the same characteristic fit as a function of gauge length for all other fibre types.

The fit of the simple Weibull distribution to trilobal fibre data is illustrated in Fig. 6. While the parameter set yields an adequate description at the middle gauge length, the Weibull quantity is underestimated at the shorter gauge length and overestimated at the longer gauge length. Figs 7–9 illustrate that while the higher order models proposed by Johnson gave improved MLFs, they suffered from the same deficiency. This also proved true for all other fibre types.

While Beetz's adaptation [13] of the exclusive model has the disadvantage of containing a parameter which must be adjusted with gauge length, the earlier discussion of his work illustrates that useful insights can be obtained from fitting such a model. With three

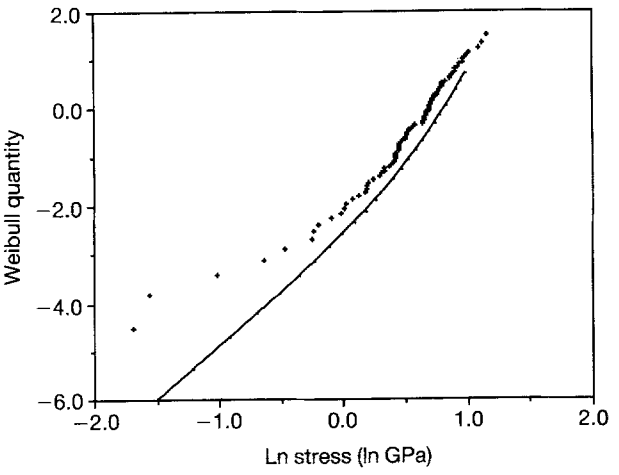

Figure 7 Concurrent distribution fit to trilobal fibre data, equivalent thickness study, 10 mm gauge length.

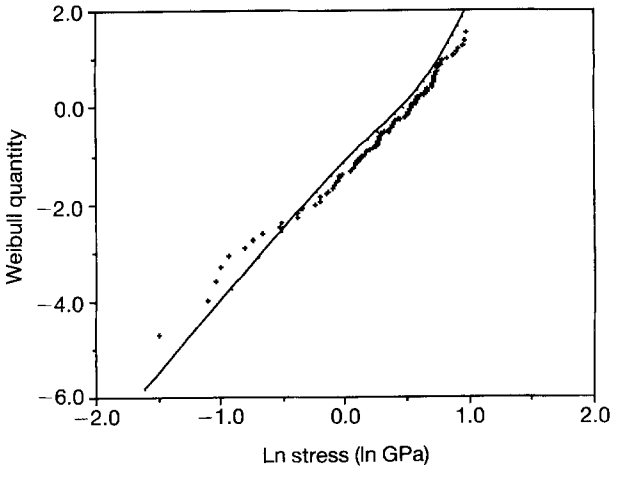

Figure 8 Exclusive distribution fit to trilobal fibre data, equivalent thickness study, 40 mm gauge length.

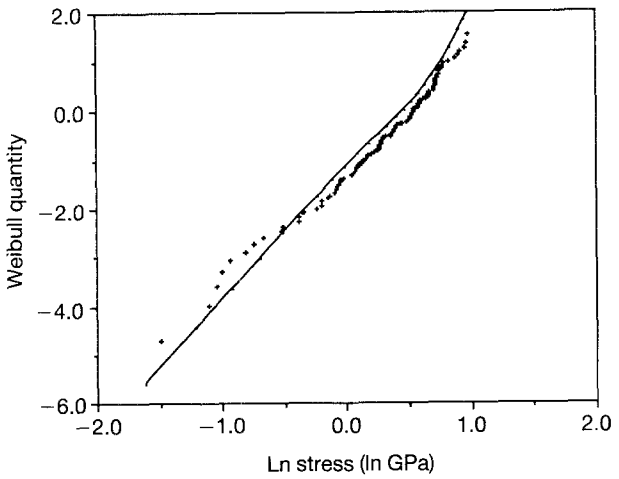

Figure 9 Partially concurrent distribution fit to trilobal fibre data, equivalent thickness study, 40 mm gauge length.

TABLE IV Results of applying Beetz's model [13] to round and trilobal fibre tensile data

Fibre shape/study	Gauge length, L (mm)	x	$\bar{\sigma}_1$ (GPa)	$\bar{\sigma}_2$ (GPa)
Round, equivalent area	10	1.00	2.14	2.50
	20	0.41	1.89	2.20
	40	0.00	1.68	1.93
Trilobal, equivalent area	10	0.84	1.70	2.00
	20	0.34	1.45	1.74
	40	0.00	1.24	1.51
Round, equivalent thickness	10	1.00	2.15	2.91
	20	0.79	1.77	2.58
	40	0.53	1.46	2.28
Trilobal, equivalent thickness	10	1.00	1.75	2.35
	20	0.73	1.40	2.08
	40	0.51	1.12	1.84

gauge lengths and four Weibull parameters, this model required the fitting of seven parameters to the data for each fibre type. The results obtained in this study, which are presented in Table IV, were very similar to those obtained by Beetz [13]. The most severe flaw population (lowest mean strength) demonstrated a decreasing mixing parameter (i.e. less relative effect) as gauge length increased. Because this is more consistent with the nature of end effects rather than a true flaw population, the end-effect model was developed and applied to the experimental data.

The fit of this model is illustrated for each fibre type in Figs 10–13. As seen in the figures, the model provided an excellent description of the experimental data over the range of gauge lengths studied. A T-ratio test, developed by Nelson [9] for comparing different models on the basis of MLF values and number of parameters required, was also applied to these results [1]. For each fibre type, the end-effect model provided a significantly better fit than all other models.

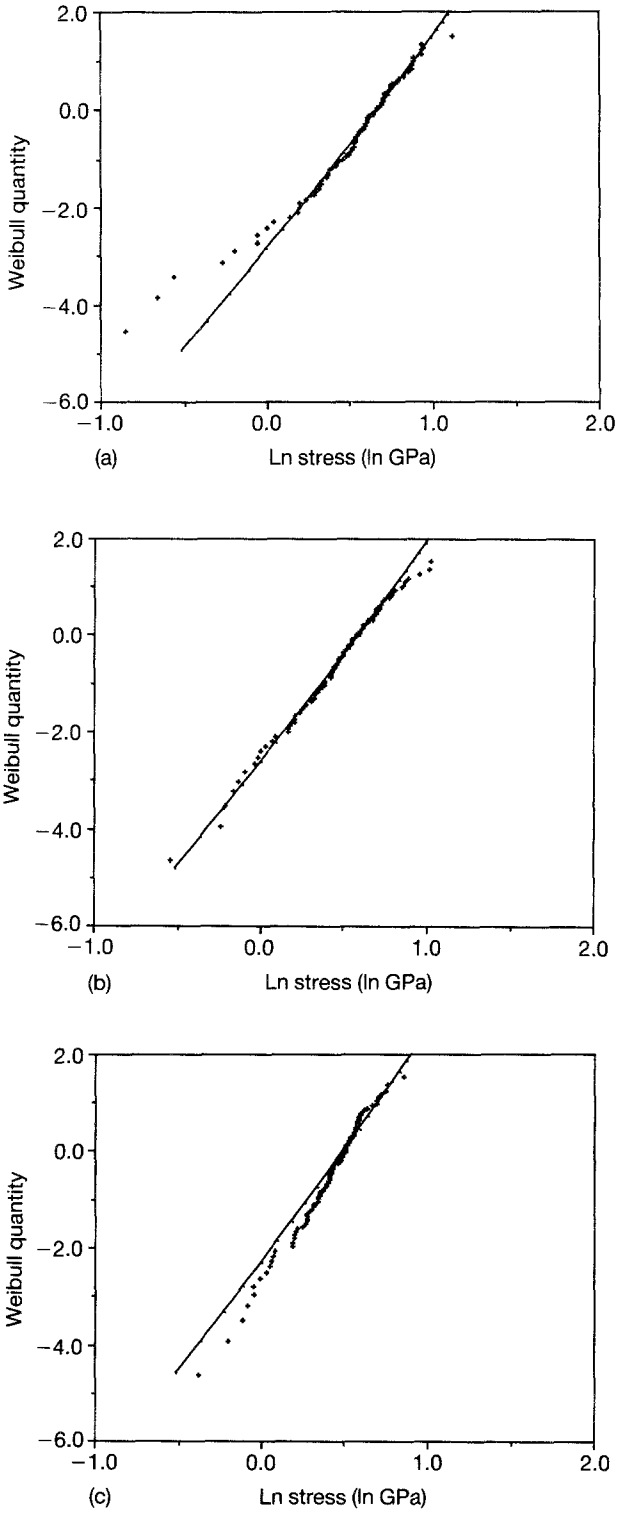

Figure 10 End-effect model fit to trilobal fibre data, equivalent area study: (a) 10 mm gauge length; (b) 20 mm gauge length; (c) 40 mm gauge length.

One advantage of the end-effect model is that the survival probabilities S_1 and S_2 can be studied separately to examine the impact of end effects on the experimental data or to separate end effects from the true strength distribution. An interesting example of this appears in Fig. 14. Here, the total survival probability was dominated by end-effect related failure rather than the true flaw population. In the case of a round fibre for the equivalent thickness study, end

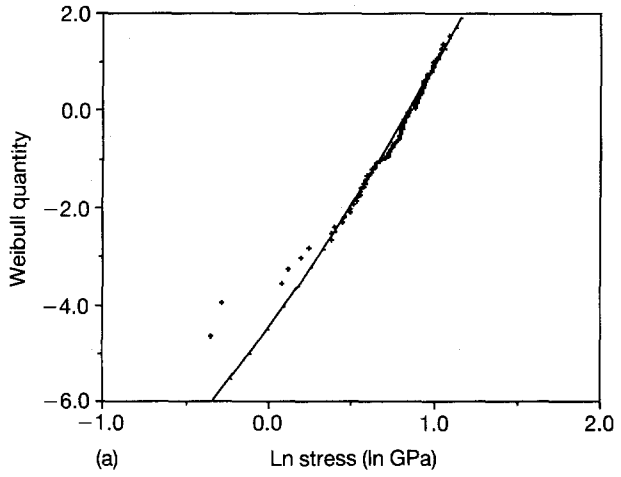

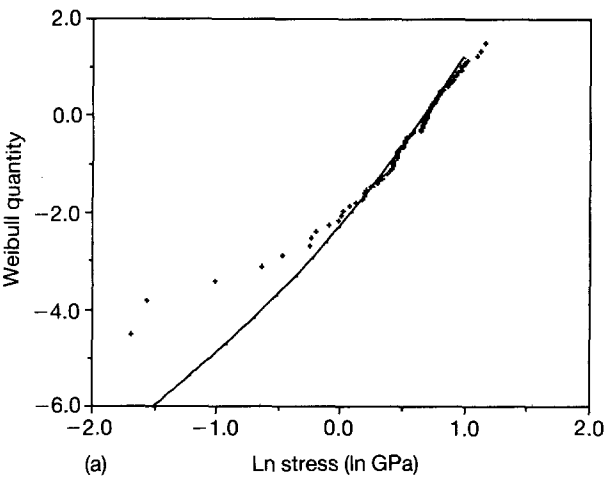

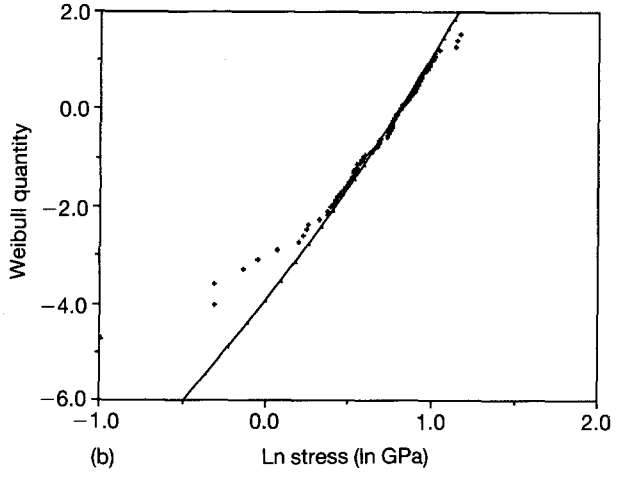

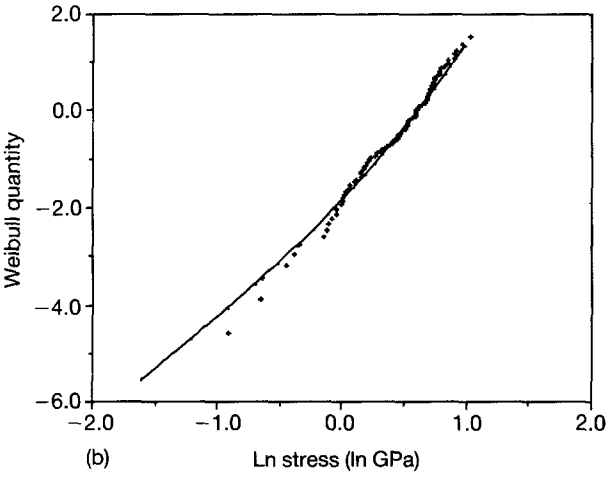

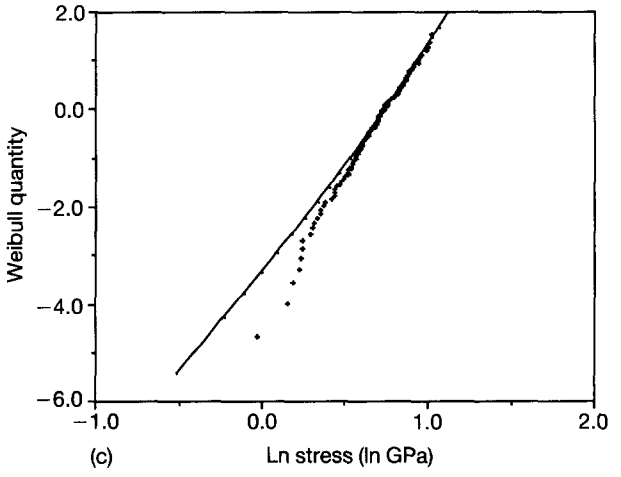

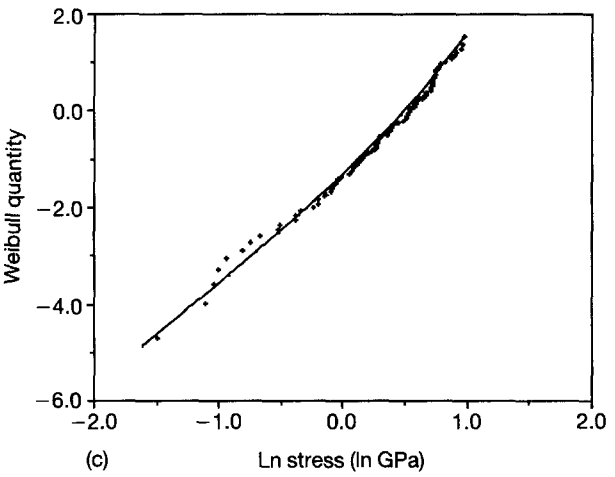

Figure 11 End-effect model fit to round fibre data, equivalent area study: (a) 10 mm gauge length; (b) 20 mm gauge length; (c) 40 mm gauge length.

Figure 12 End-effect model fit to trilobal fibre data, equivalent thickness study: (a) 10 mm gauge length; (b) 20 mm gauge length; (c) 40 mm gauge length.

effects and true flaws had nearly equal impact on data taken at a 40 mm gauge length, although one might think that end effects would be of minor importance at this gauge length.

Separation of end effects can be accomplished in other ways as well, and end-effect separation was particularly useful in comparing round and trilobal fibres. One approach used here was to calculate the average strength arising from S_1 (true flaws) alone and compare these for the fibres in each study. These results are presented in Figs 15 and 16 for the equivalent area and equivalent thickness studies, respectively. The model indicates that in both studies, the round fibre is the stronger of the two shapes and that round and trilobal fibres in the equivalent area study exhibit similar dependencies of strength on gauge length. However, it should be noted that the average cross-sectional area of the trilobal fibre was a factor of

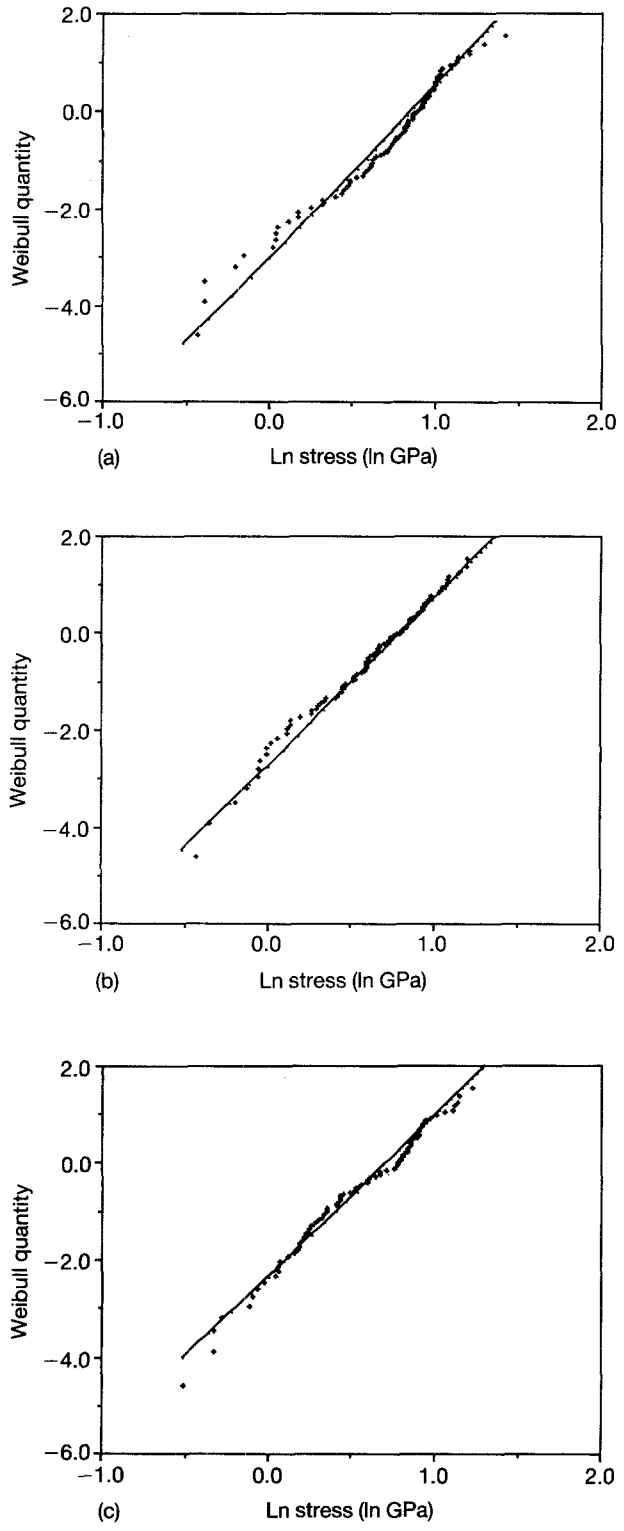

Figure 13 End-effect model fit to round fibre data, equivalent thickness study: (a) 10 mm gauge length; (b) 20 mm gauge length; (c) 40 mm gauge length.

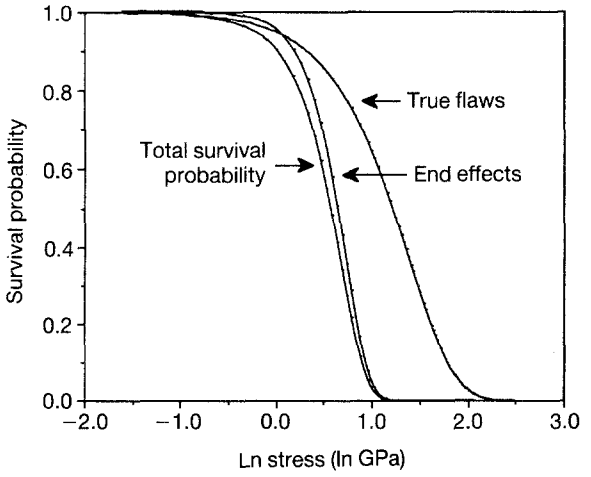

Figure 14 Influence of end effects and true flaws on total survival probability, trilobal fibre data, equivalent thickness study, 10 mm gauge length.

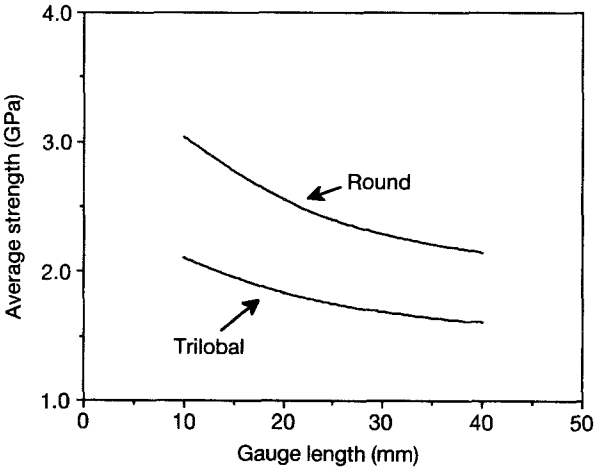

Figure 15 Average strength associated with true flaws for round and trilobal fibres of equivalent area.

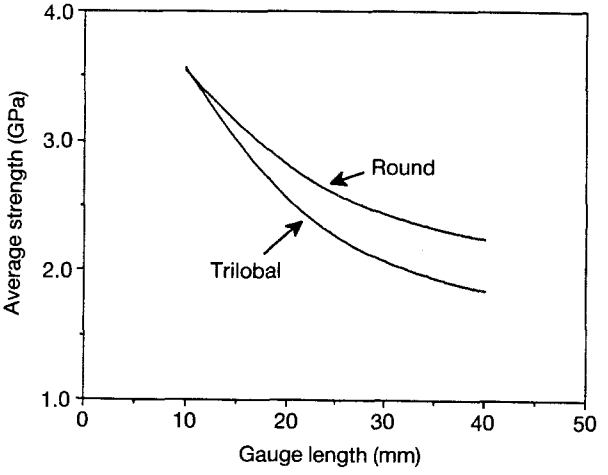

Figure 16 Average strength associated with true flaws for round and trilobal fibres of equivalent thickness.

five larger than that of round fibres in the equivalent thickness study. Because larger fibres are easier to spin, it appears that trilobal fibres do offer the advantage of competitive properties and simpler processing at large cross-sectional areas, whereas large round fibres would be difficult, if not impossible, to stabilize properly.

5. Conclusions

In the current work, an end-effect model has been developed to describe single-filament data for brittle fibres. This model is based on sound physical reason-

ing and accounts for a known inadequacy of the test method. The model provides a significantly better fit of the experimental data than does the simple Weibull distribution and a number of mixed distributions based on the Weibull. The results obtained here indicate end effects to be of critical importance at gauge lengths of 10 mm and shorter, and in some cases, at gauge lengths as long as 40 mm. The fitted model is easily used to separate end effects from the true fibre strength distribution, and the ability to do this is critical for comparative studies of brittle fibres. In this work, use of the model revealed no significant differences in attainable strengths for fibres of different shapes. Rather, the advantage of alternate fibre cross-sectional geometries lies in a decreased sensitivity of fibre properties to fibre size as compared to conventional round fibres.

Acknowledgements

The authors thank the National Science Foundation (grant number 8710385) and the Air Force Office of Scientific Research (grant number S-789-000-015) for supporting this research.

References

1. J. B. JONES, J. B. BARR and R. E. SMITH, *J. Mater. Sci.* **15** (1980) 2465.
2. D. D. EDIE, N. K. FOX, B. C. BARNETT and C. C. FAIN, *Carbon* **24** (1986) 477.
3. H. E. GAINEY, D. D. EDIE, J. M. KENNEDY and C. C. FAIN, "Carbon 88", Proceedings of the Seventh International Carbon Conference, Newcastle, UK edited by B. McEnaney and T. J. Mays (IOP, Bristol, 1988) p. 494.
4. E. G. STONER, PhD dissertation, Clemson University, Clemson, SC (1991).
5. ASTM Standard, D3379-75, Reapproved 1989 (American Society for Testing and Materials, Philadelphia, PA).
6. J. W. HITCHONS and D. C. PHILLIPS, *Fibre Sci. Technol.* **12** (1979) 217.
7. C. P. BEETZ, Jr. *ibid.* **16** (1982) 45.
8. H. D. WAGNER and S. L. PHOENIX, *J. Compos. Mater.* **18** (1984) 312.
9. W. NELSON, "Applied Life Data Analysis" (Wiley, New York, 1982).
10. K. K. PHANI, *J. Mater. Sci.* **6** (1987) 1176.
11. *Idem, ibid.* **23** (1988) 1189.
12. C. A. JOHNSON, in "Fracture Mechanics of Ceramics 5" edited by R. C. Bradt, A. G. Evans, D. P. H. Hasselman and F. F. Lange (Plenum Press, New York, 1985) pp. 365–86.
13. C. P. BEETZ, Jr, *Fibre Sci. Technol.* **16** (1982) 81.
14. L. S. SINGER, US Pat. 4005 183 (1977).

Received 2 April 1993
and accepted 27 May 1994